

# River network response to thrust sheet propagation into a foreland

Yutong Jiang<sup>1</sup>, Yanyan Wang<sup>2</sup>, Sean D. Willett<sup>2</sup>, and Honghua Lu<sup>1</sup>

<sup>1</sup> School of Geographic Sciences, East China Normal University, Shanghai, China

<sup>2</sup> Department of Earth and Planetary Sciences, ETH Zurich, Zurich, Switzerland

## 1. Motivation

Tian Shan Thrust Sheet Propagation and Surface Uplift: Active deformation in the Tian Shan offers a clear case of ongoing thrust sheet propagation and associated surface uplift, providing insight into dynamic orogenic processes.

Impact of Tectonics on River Systems: Observable drainage reorganization, such as river diversion along fault zones, raises questions about how tectonic activity shapes fluvial systems over time.

Modeling Tectonics and River Evolution: The study uses the DAC model to simulate the effects of thrust sheet propagation on drainage networks, linking tectonics with landscape evolution.

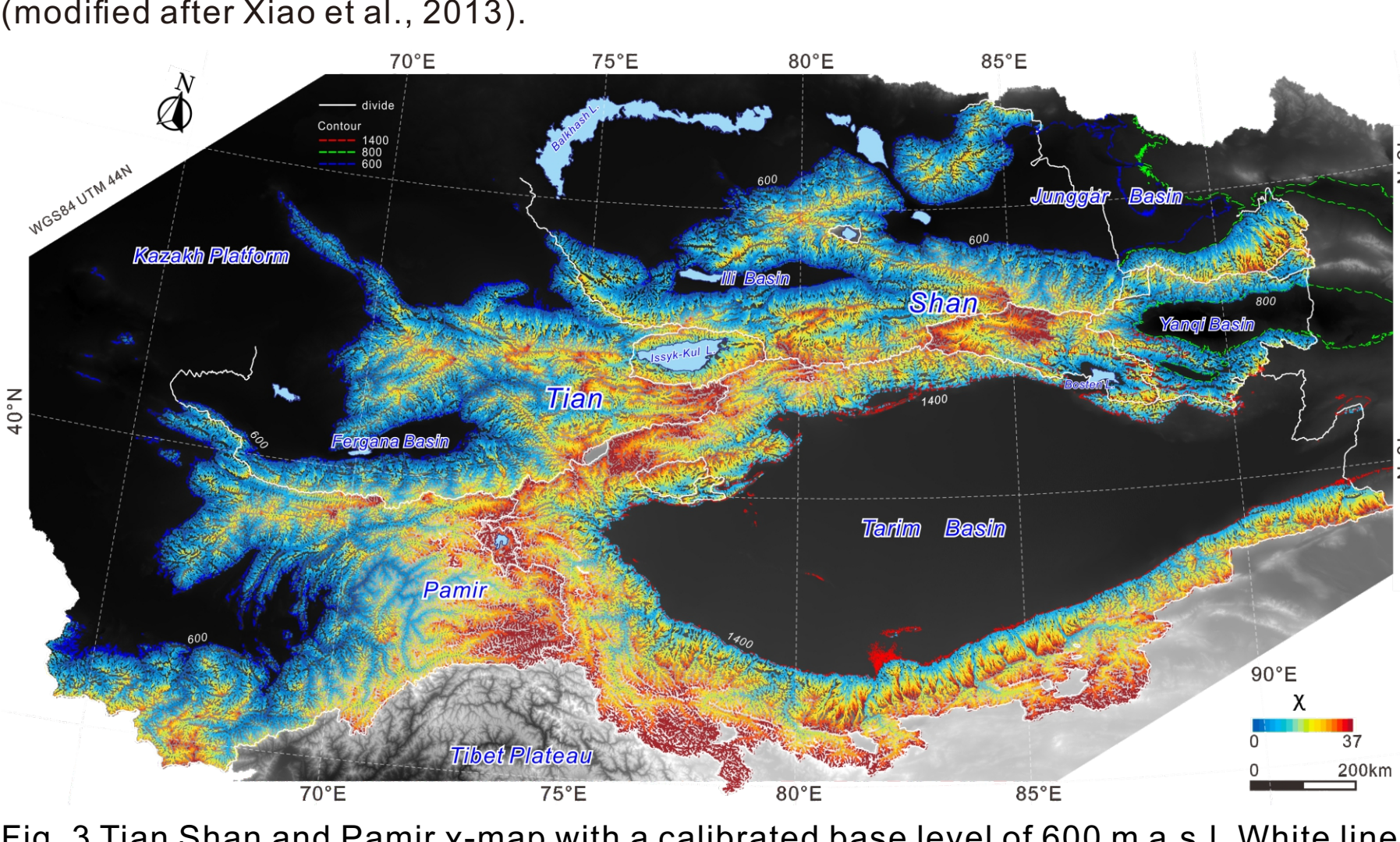
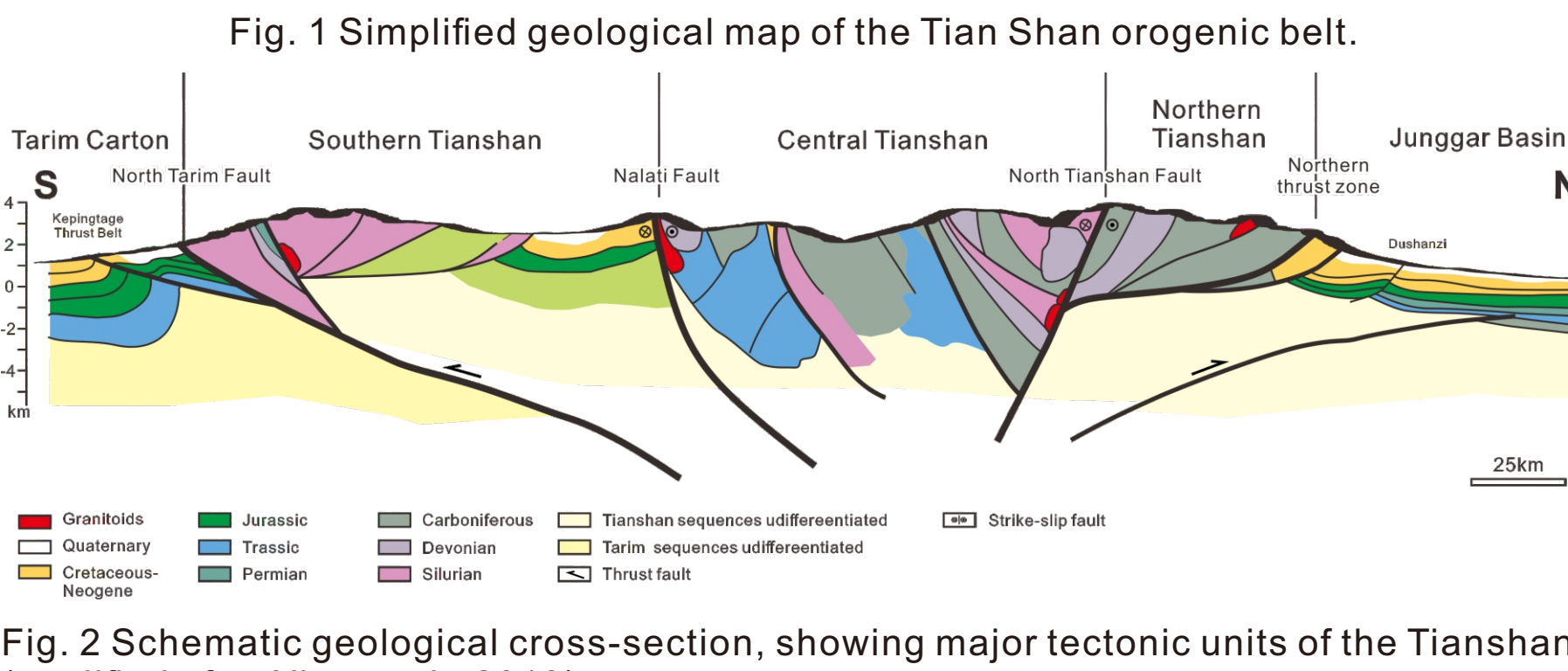
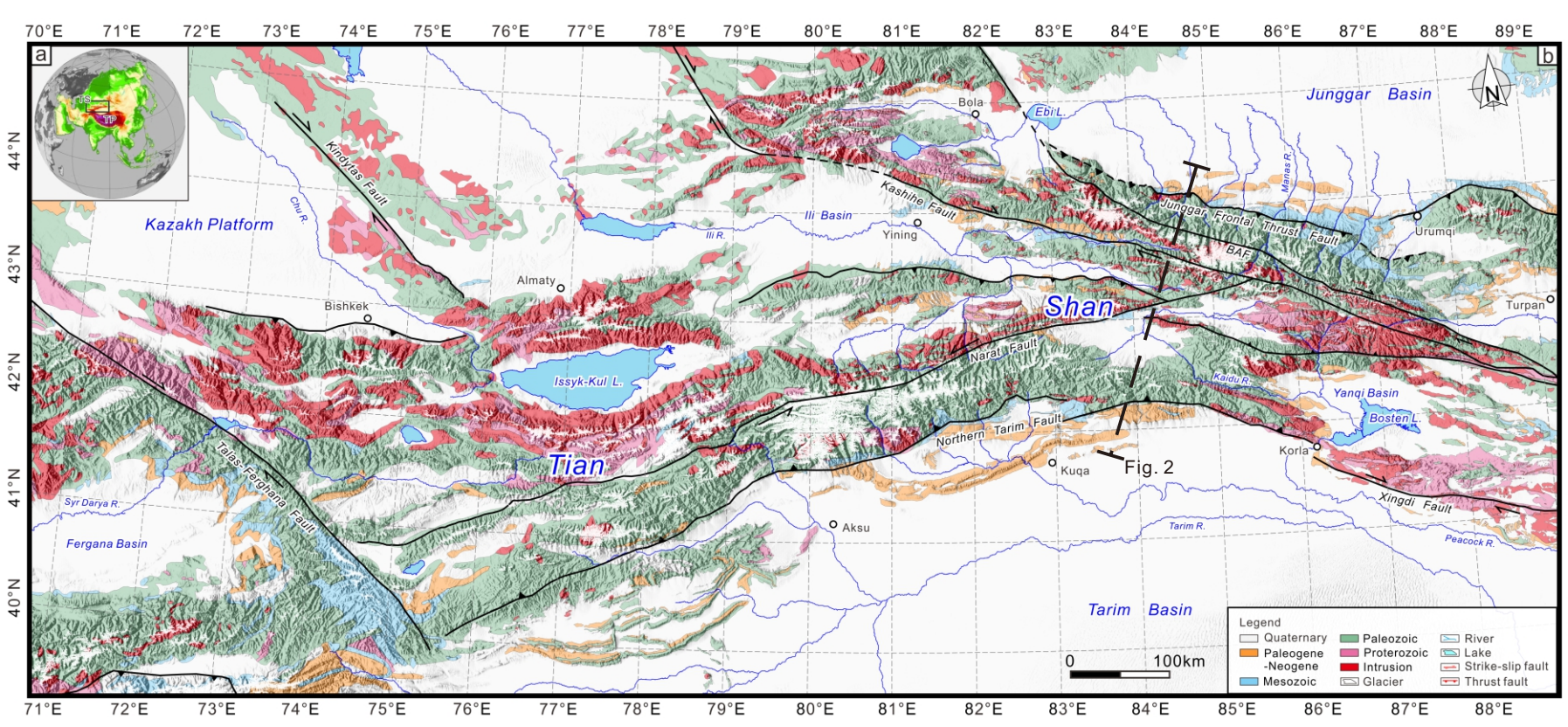


Fig. 1 Simplified geological map of the Tian Shan orogenic belt.

Fig. 2 Schematic geological cross-section, showing major tectonic units of the Tianshan (modified after Xiao et al., 2013).

Fig. 3 Tian Shan and Pamir x-map with a calibrated base level of 600 m a.s.l. White lines refer to the main river catchment outlines. Note large and common disequilibrium basin geometry and many lakes and closed basins

### Questions:

- How do intermountane basins form?
- How long do basins persist?
- How does longitudinal drainage develop?

## 2. Methods

The landscape evolution model, Divide and Capture (DAC) (Goren et al., 2014), combines a numerical solver for fluvial incision over a triangular, irregular, and sparse grid, with analytical solutions for the fluvial and hillslope topography at the sub-grid scale. The numerical solver implements the stream-power law (Whipple & Tucker, 1999):

$$E = KA^nS^m \quad (1)$$

The river erosion rate,  $E$ , is physically characterized by the stream power on the substrate and rock erodibility,  $K$ . Stream power is determined by the drainage area,  $A$ , and channel slope,  $S$ .  $m$  and  $n$  are empirical parameters.

In this study, a 200x150 km rectangular domain was defined, which had its edges at a constant elevation. It was assumed that the slope index ( $n$ ) was 1, the area index ( $m$ ) was 0.495. We present three models. For the reference model, the background uplift rate ( $U$ ) was  $2 \times 10^{-5}$  m/yr, and erodibility ( $K$ ) was  $2 \times 10^{-6}$  m $^{0.01}$ /yr. Two contrasting models were constructed with different  $K$ ;  $U$  was changed to hold  $U/K$  constant. This holds topography constant, but changes the sediment flux. Steady-state topography was generated using the initial random elevation field, assuming the initial structural uplift rate was uniform in space, without horizontal motion. After forming a symmetrical mountain range with a maximum elevation of 500 m, vertical uplift was imposed to represent mountain building.

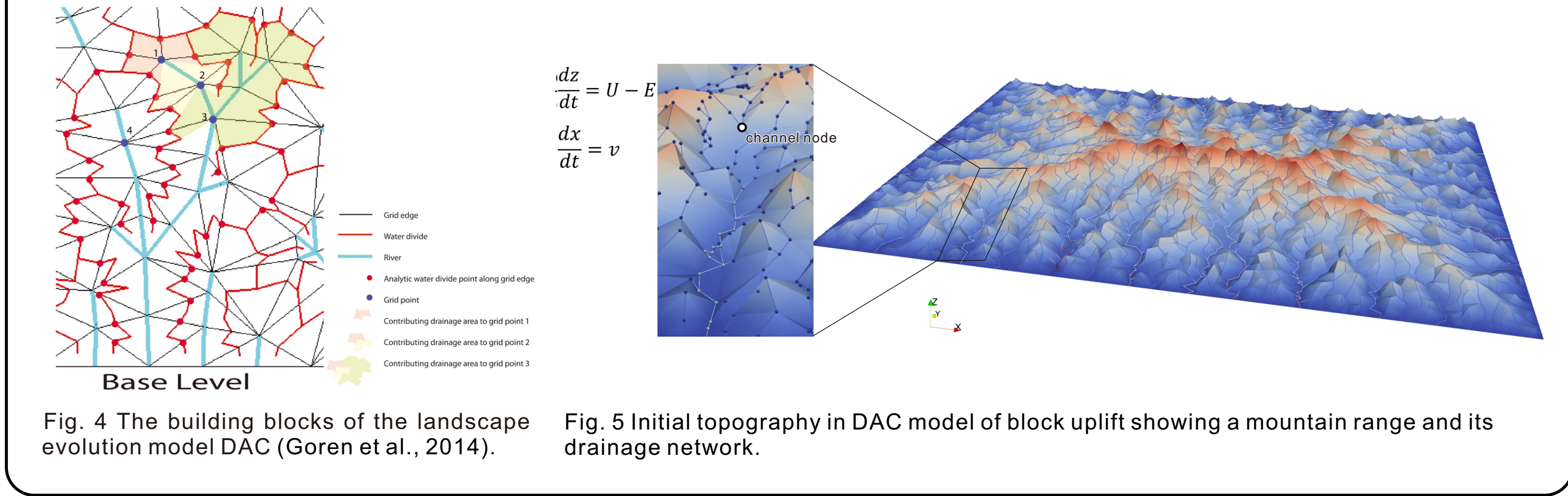


Fig. 4 The building blocks of the landscape evolution model DAC (Goren et al., 2014).

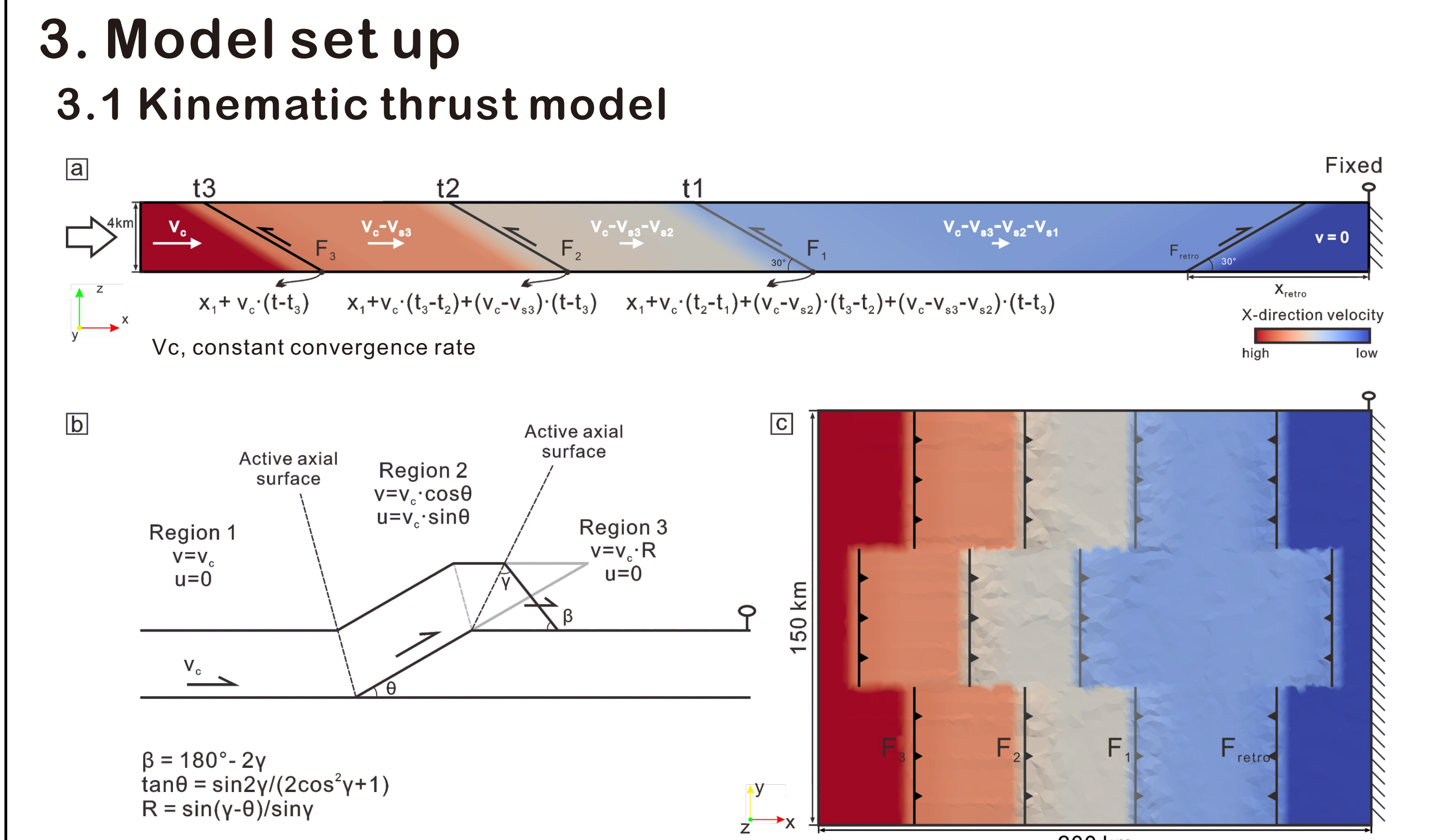


Fig. 6 Model configuration. (a) Cross-section view of the structural model showing convergence partitioning on thrust fault segments. Convergence velocity,  $V_c$  is constant for all time and across all models. White arrows represent the x direction velocity  $v_{x1}$ ,  $v_{x2}$  and  $v_{x3}$  absorbed by each thrust fault. The color shows the rock velocity of different regions. Thrust faults move with their footwalls. (b) The velocity model of fault-bend folding (modified after Hardy et al., 1995). Uplift rate,  $U$  is determined by fault geometry. (c) Downward view of domain after all faults are activated (200x150km). The pro-wedge thrust fault propagates towards left, while the retro-wedge thrust fault does not propagate and the right side boundary is fixed. Faults are activated in sequence at times  $t_1$ ,  $t_2$  and  $t_3$ .

## 3. Model set up

### 3.1 Kinematic thrust model

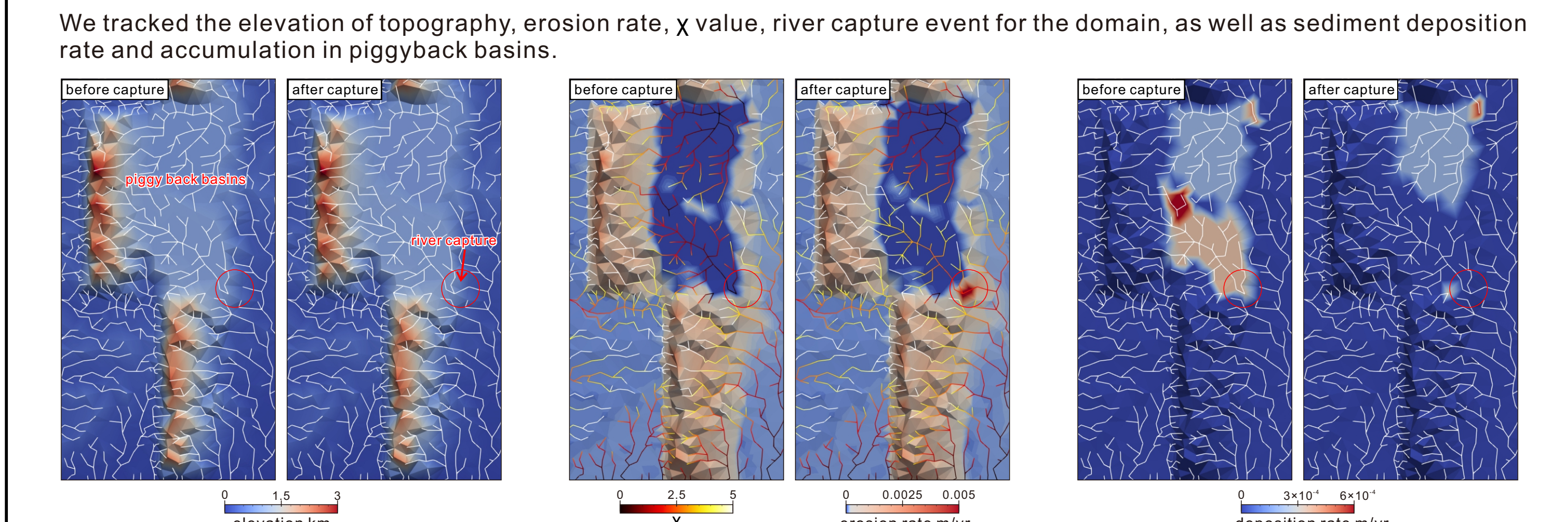


Fig. 7 Example river capture event showing the difference before and after capture.

## 2. Methods

The landscape evolution model, Divide and Capture (DAC) (Goren et al., 2014), combines a numerical solver for fluvial incision over a triangular, irregular, and sparse grid, with analytical solutions for the fluvial and hillslope topography at the sub-grid scale. The numerical solver implements the stream-power law (Whipple & Tucker, 1999):

$$E = KA^nS^m \quad (1)$$

The river erosion rate,  $E$ , is physically characterized by the stream power on the substrate and rock erodibility,  $K$ . Stream power is determined by the drainage area,  $A$ , and channel slope,  $S$ .  $m$  and  $n$  are empirical parameters.

In this study, a 200x150 km rectangular domain was defined, which had its edges at a constant elevation. It was assumed that the slope index ( $n$ ) was 1, the area index ( $m$ ) was 0.495. We present three models. For the reference model, the background uplift rate ( $U$ ) was  $2 \times 10^{-5}$  m/yr, and erodibility ( $K$ ) was  $2 \times 10^{-6}$  m $^{0.01}$ /yr. Two contrasting models were constructed with different  $K$ ;  $U$  was changed to hold  $U/K$  constant. This holds topography constant, but changes the sediment flux. Steady-state topography was generated using the initial random elevation field, assuming the initial structural uplift rate was uniform in space, without horizontal motion. After forming a symmetrical mountain range with a maximum elevation of 500 m, vertical uplift was imposed to represent mountain building.

### 3.3 Sensitivity test

Parameters	Description	Model 1	Model 2	Model 3	Unit
$K$	Erodibility	$1 \times 10^{-6}$	$2 \times 10^{-6}$	$4 \times 10^{-6}$	$\text{m}^{0.01}/\text{yr}$
$U$	Background uplift rate	$5 \times 10^{-5}$	$1 \times 10^{-4}$	$2 \times 10^{-4}$	$\text{m}/\text{yr}$
$V_c$	Total convergence velocity	$2 \times 10^{-3}$	$4 \times 10^{-3}$	$8 \times 10^{-3}$	$\text{m}/\text{yr}$
$V_{\text{retro}}$	Shortening rate of retro-wedge	$5 \times 10^{-4}$	$1 \times 10^{-3}$	$2 \times 10^{-3}$	$\text{m}/\text{yr}$
$V_s$	Shortening rate of pro-wedge	$(V_c - V_{\text{retro}})/N$			$\text{m}/\text{yr}$
$V_f$	Slip rate of thrust faults	$V_{\text{retro}}/\cos\theta$ for retro-wedge, $V_c/\cos\theta$ for pro-wedge			$\text{m}/\text{yr}$

\*  $N$ , number of active thrust faults on pro-wedge.  $\theta = 30^\circ$ , dip angle of the thrust faults.

## 4. Results

### 4.1 Time sequences of reference model (Model 2)

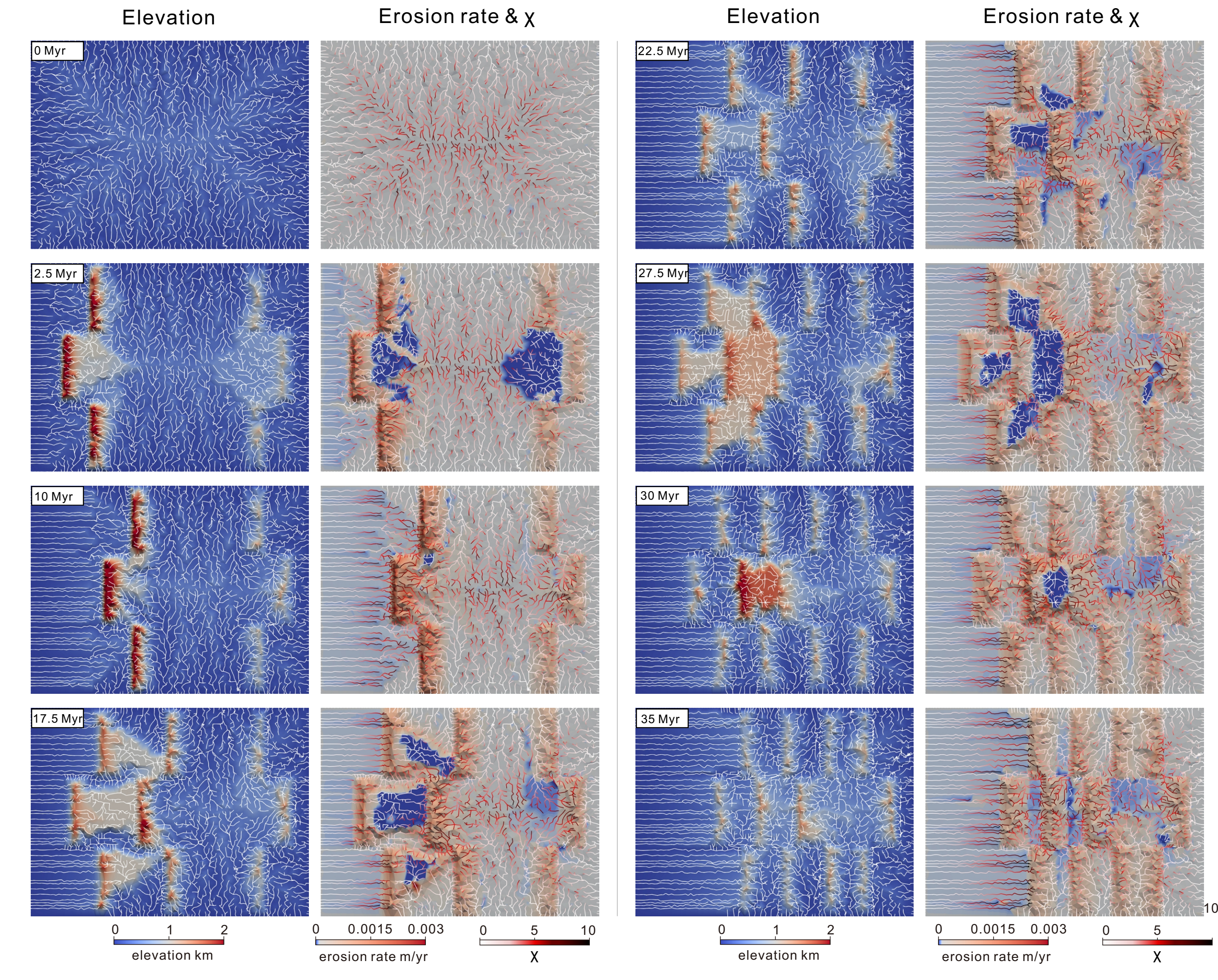


Fig. 8 Topography and erosion rate for the reference model (Model 2) from initial topography-0 Ma to 35 Ma. Note that erosion rate of zero represents sediment deposition.

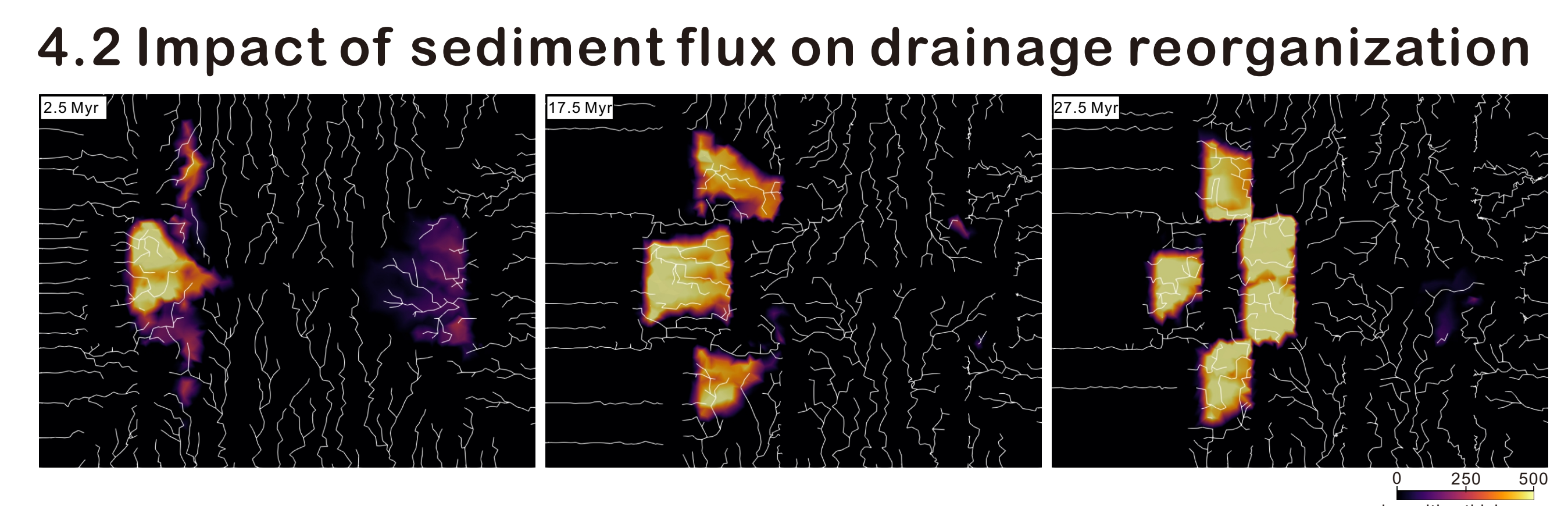


Fig. 9 Deposition thickness of model 2 at 2.5, 17.5 and 27.5 Myr, the elevation and erosion rate are shown in Fig. 8.

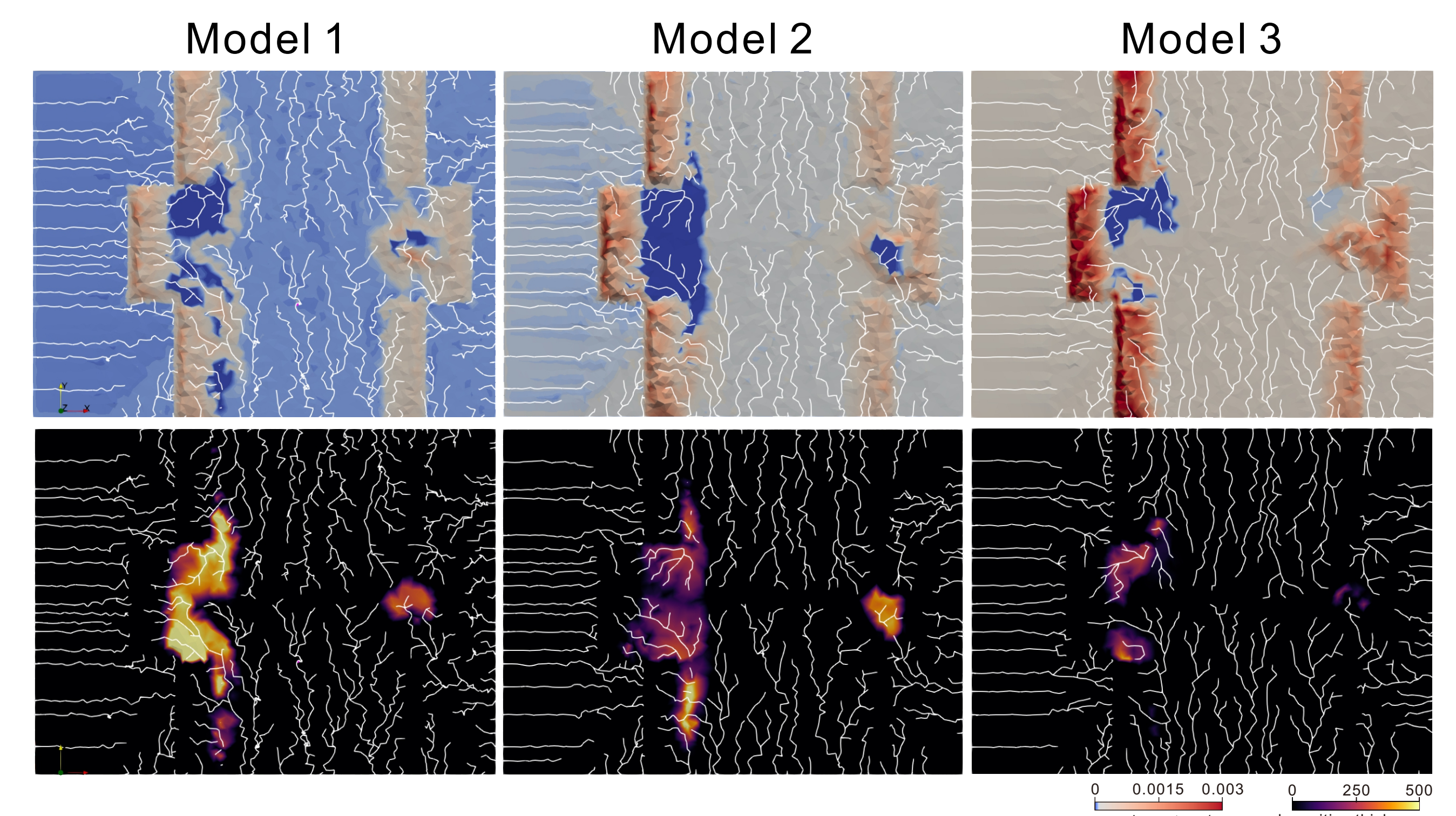


Fig. 10 Erosion rate and deposition thickness at 7.75 Myr of model 1, 2 and 3, which shows a time lag for basin formation with higher  $U$  and  $K$ , implying higher sedimentation rate.

### 4.3 Deposition in intermountainous basins

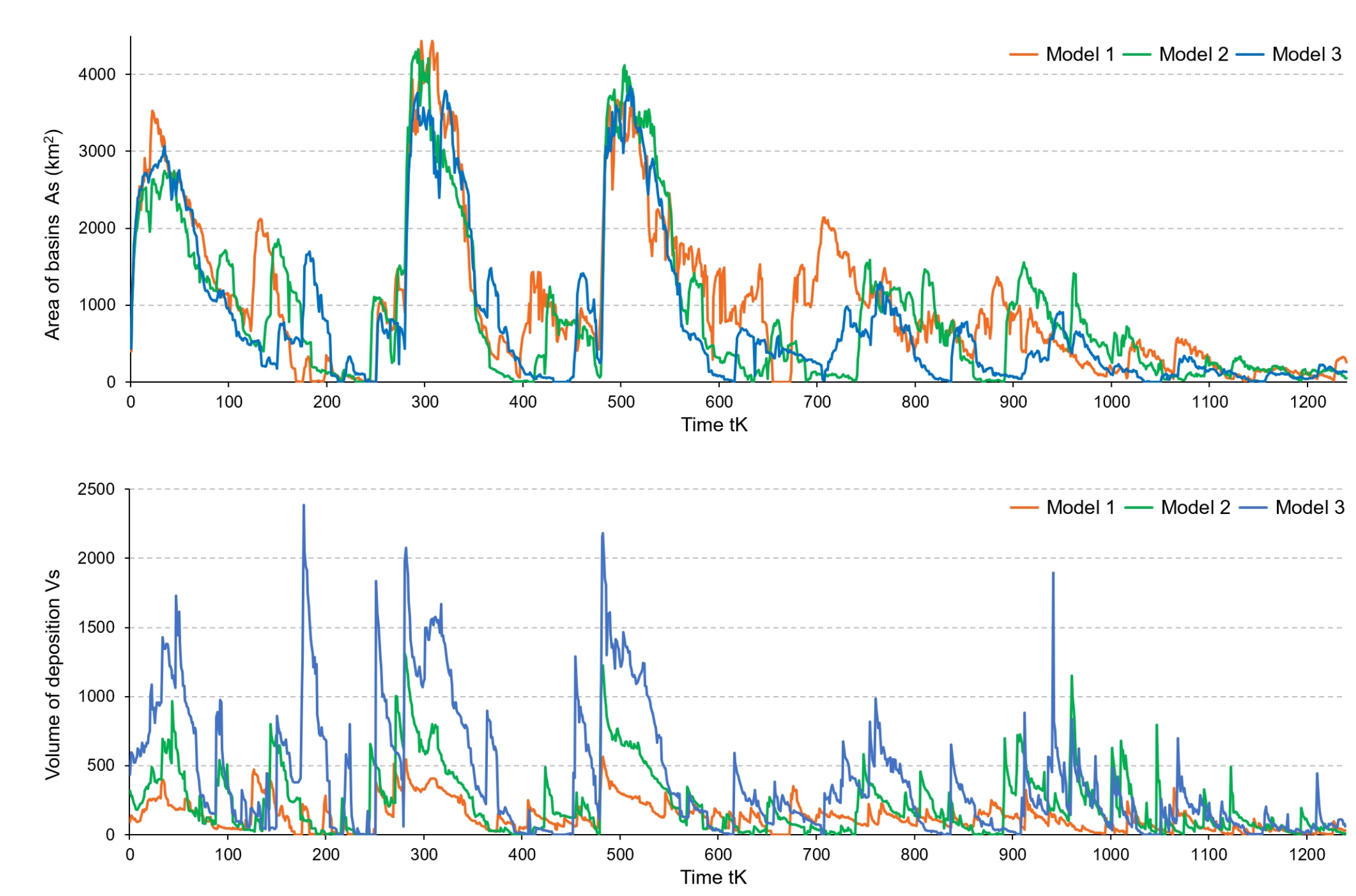


Fig. 11 Total sedimentary basin area and volume of deposition. The time  $tK$  is non-dimensional to allow for easier comparison.

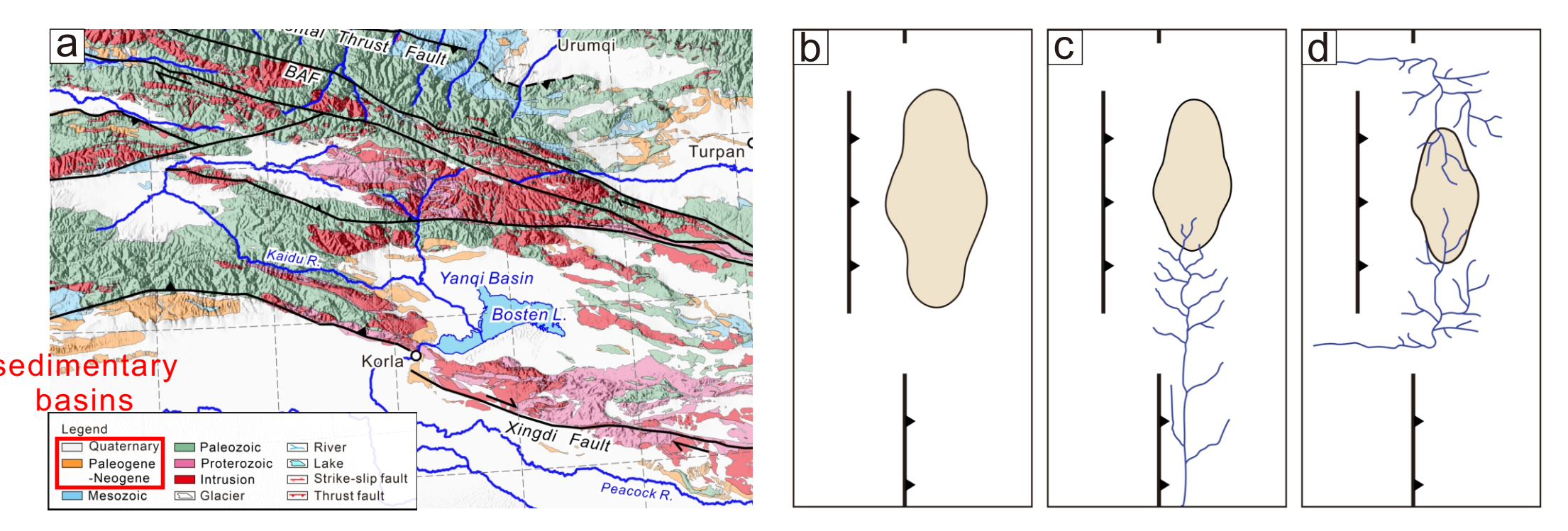


Fig. 12 (a) Example basins in Tian Shan (b) Formation and destruction of piggyback basins. (c) re-integration by lateral river. (d) re-integration by foreland river



## 5. Conclusions

- Piggyback basins form where thrust defeat foreland rivers
- Basins are always transient
- Formation and longevity of basins is encouraged by high sediment flux
- Re-integration of basins occurs by river capture from lateral boundaries when open
- Re-integration can occur to foreland only when lateral drainage is impeded

## References

- [1] Goren L., Willett S.D., Herman F. et al. (2014). Coupled numerical-analytical approach to landscape evolution modeling. *Earth Surf. Process. Landf.*, 39(4), 522–545.
- [2] Hardy S., Poblet J. et al. (1995). The velocity description of deformation, paper 2: sediment geometries associated with fault-bend and fault-propagation folds. *Mar. Pet. Geol.*, 12(2), 165–176.
- [3] Whipple, K. X., & Tucker, G. E. (1999). Dynamics of the stream-power river incision model: Implications for height limits of mountain ranges, landscape response timescales, and research needs. *J. Geophys. Res.*, 104(B8), 17661–17674.
- [4] Xiao W.J., Windley B.F., Allen M.B. et al. (2013). Paleozoic multiple accretionary and collisional tectonics of the Chinese Tianshan orogenic collage. *Gondwana Res.*, 23(4), 1316–1341.